Photodissociation of Spatially Aligned Acetaldehyde Cations†

Suk Kyoung Lee,‡,§ Ruchira Silva,‡ Myung Hwa Kim,‡,§ Lei Shen,‡ and Arthur G. Suits*,‡,§

Department of Chemistry, Wayne State University, Detroit, Michigan 48202, and Department of Chemistry, Stony Brook University, Stony Brook, New York 11794

Received: November 20, 2006; In Final Form: January 4, 2007

Photofragment translational energy and angular distributions are reported for the photodissociation of acetaldehyde cations in the wavelength range 354−363 nm obtained using the DC slice ion imaging technique. Vibrationally selected parent ions were produced by 2+1 resonance-enhanced multiphoton ionization (REMPI) via the 3s ← n Rydberg transition, with photodissociation resulting from absorption of a fourth additional photon. Three product channels were observed: HCO^+, CH_3CO^+, and CH_4^+. The angular distributions reveal that all product channels have a predominantly parallel recoil anisotropy although the lower β_2 parameter of CH_3CO^+ indicates the concomitant presence of a perpendicular component. Furthermore, the distinct angular distribution of the CH_3CO^+ fragments shows a large value of the higher order Legendre polynomial term, providing evidence that acetaldehyde cations are spatially aligned during the ionization process.

I. Introduction

The photofragmentation processes of cations provide an avenue to investigate a number of important issues in photochemistry. Cations prepared from closed-shell neutrals are open-shell systems, so many low-lying electronic states exist and interactions among them may be readily explored; resonant ionization techniques may be used to prepare specific vibrational states or even particular molecular conformers for photochemical studies, and vibrationally mediated or mode-specific dissociation may be seen; finally, quantum control experiments often probe fragmentation processes in the product ions, so understanding the neutral and ionic pathways leading to the same final ionic product may be important. Ion imaging represents a powerful means of examining photofragmentation processes in ions. Recently, the photodissociation processes of cations have been extensively explored by velocity map imaging,[1−3] slice imaging,[4,5] and reflectron multimass velocity map imaging[6,7] methods combined with REMPI. The advantage of the imaging technique in these applications is the ability to measure the translational energy and angular distributions easily and with great sensitivity. In addition, the sensitivity of the angular distribution to the symmetry and lifetime of the intermediate state may be important to understand complicated dynamical processes.

The photodissociation of acetaldehyde cations formed by either vacuum-ultraviolet (VUV) or multiphoton ionization has been studied using ionization mass spectrometry,[8,9] photoelectron-photoion coincidence spectrometry,[10,11] and the Fourier transform ion cyclotron resonance (FT-ICR) technique.[12] Bombach et al.[10] reported that CH_3CO^+ and HCO^+ are produced either by internal conversion to the ground electronic state ($\tilde{X}^2A'$) of acetaldehyde cations (95%) or by isomerization to ground state oxirane (5%) near the onset of the $\tilde{A}^2A''$ band. The photoelectron-photoion coincidence studies of Johnson and co-workers[11] showed that CH_4^+ appears together with CH_3CO^+ and HCO^+ above an ionization energy of 13 eV, and the formation of CH_4^+ was interpreted as characteristic of dissociation through the $\tilde{A}^2A''$ band. In the $\tilde{B}^2A'$ band above 14.1 eV, CH_3^+ starts to emerge in addition to CH_3CO^+ and HCO^+, along with a decreasing abundance of CH_4^+. The translational energy distribution of the acetyl ion was cited as evidence that CH_3^+ is produced via secondary fragmentation of CH_3CO^+.[11] Fisanick et al.[9] and Shin et al.[12] proposed that the photodissociation of acetaldehyde cations prepared by multiphoton ionization takes place predominantly by excitation to the $\tilde{B}^2A'$ state. An energy diagram is shown in Figure 1 illustrating the relevant multiphoton ionization and dissociation processes.

In this report, parent ions were generated by 2+1 REMPI through the B^1A' state corresponding to the 3s ← n Rydberg transitions in the range from 354 to 363 nm. The wealth of spectroscopic knowledge for these Rydberg states[13−17] allows identification of the vibrational states of parent ions and thus provides a way to elucidate the effect of mode-selective vibrational excitation on cation photodissociation processes. Based on thermodynamic data taken from ref 18, four dissociation processes, leading to CH_3CO^+, HCO^+, CH_4^+, and CH_3^+ products, are energetically possible with four photons in this wavelength range (Figure 1). Shin et al.[12] observed only acetyl ions and formyl ions in this energy region, but Fisanick et al.[9] detected several product ions that can be formed with the absorption of up to five photons at the origin band of Rydberg state. A strong power dependence of fragment ion production was also reported in that case.[9]

In the following pages, we present results of an imaging study of the photodissociation of specific vibrational levels of acetaldehyde cations prepared by following 2+1 REMPI. Particular emphasis is placed on the use of the angular distributions to gain insight into the electronic transitions responsible and to investigate the extent of spatial alignment of the parent ions produced in the REMPI excitation.

II. Experimental Section

The overall experimental apparatus employed in the DC slice imaging approach has been described in detail elsewhere,[19] so only a brief sketch will be given here. A pulsed supersonic

† Part of the special issue "M. C. Lin Festschrift".

* Corresponding author. E-mail: asuits@chem.wayne.edu.
‡ Wayne State University.
§ Stony Brook University.

10.1021/jp067706l CCC: $37.00
Published on Web 03/28/2007

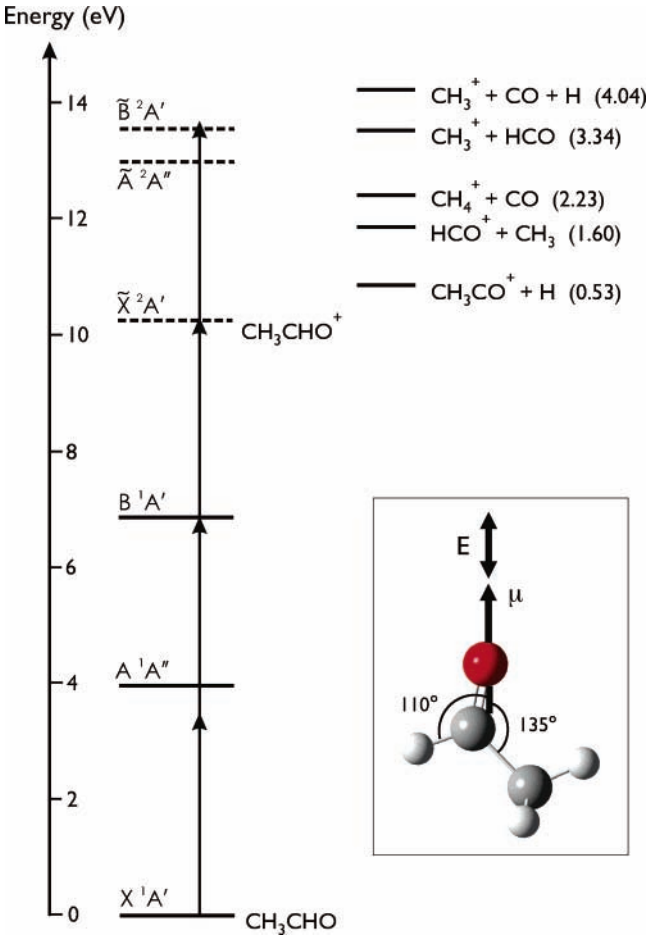

Figure 1. Schematic energy diagram for possible dissociation pathways of CH_3CHO^+ and 2+1 resonance-enhanced multiphoton ionization of CH_3CHO. The number in a parentheses indicates the dissociation threshold (eV) from acetaldehyde cation. The inset shows the orientation of the transition dipole moment for $\tilde{B} \leftarrow \tilde{X}$ excitation.

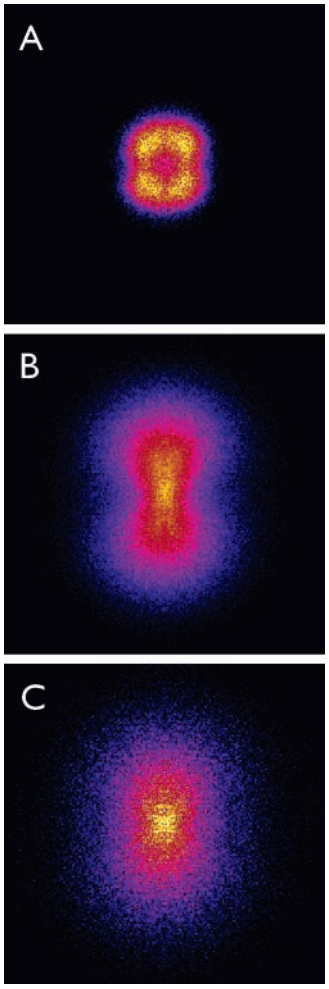

Figure 2. Experimental sliced images of three fragments (A, CH_3CO^+; B, HCO^+; C, CH_4^+) in the photodissociation of acetaldehyde cation prepared by 2+1 REMPI via the origin transition.

molecular beam of acetaldehyde seeded 24% in Ar was expanded into the source chamber and collimated by a skimmer. The beam entered into a velocity mapping electrode assembly optimized for DC slice imaging and was intersected at a right angle by a laser beam tuned to a two-photon resonant excitation of a Rydberg state of acetaldehyde. The laser light was generated by frequency doubling the output of a dye laser (Continuum Jaguar, LDS 722 dye) pumped by the 532 nm harmonic of a second Nd:YAG laser (Quanta Ray PRO 290). The polarization of the laser beam was parallel to the detector plane, and the typical output power was ~0.3 mJ/pulse in the wavelength range from 354 to 363 nm. The laser light was then focused into the interaction region with a 40 cm focal length lens. The product ions were accelerated through the multilens velocity mapping assembly and impacted upon a dual microchannel plate array of 75 mm diameter, which was coupled to a P-47 phosphor screen. In this particular instance a repeller electrode held at 400 V was used in conjunction with three additional focusing lenses in the velocity-mapping scheme to stretch the photofragment ion cloud along the time-of-flight axis to around 400 ns. The overall flight path from the laser interaction region to the detector was 100 cm. Application of a narrow (~40 ns) time gate at the detector was then used to sample the central section of the distribution. The resulting ion image was recorded using a CCD camera (Sony XC-ST50, 768 × 494 pixels) in conjunction with the IMACQ Megapixel acquisition program[20] recently developed in our group that enabled a high-resolution real time ion counting with sub-pixel precision. The newly developed Megapixel analyzing program IMAN also was used to determine the translational energy and angular distributions. In addition, the photoelectron images were obtained with a similar experimental setup, albeit with a shorter flight path and reversed potentials. For the photoelectron imaging, the main chamber and flight path were shielded with μ-metal sheet to avoid the influence of external magnetic fields.

III. Results

The sliced images for all photofragments of acetaldehyde cations following 2+1 REMPI via the origin band (55 024 cm^{-1}) of the 3s Rydberg transition are presented in Figure 2. As shown in the energy diagram (Figure 1), four products are accessible by one-photon dissociation of the parent cation at this energy (3.41 eV), but only three ionic photofragments were observed: CH_3CO^+, HCO^+, and CH_4^+. The branching ratio of products was estimated roughly from the integrated intensity of each sliced image, which is CH_3CO^+:HCO^+:CH_4^+ = 1.0:6.0:1.5. A glance at these images shows that Figure 2A, CH_3CO^+, is distinct in several ways: it shows an apparent "hole" in the center as well as a multilobed structure.

The translational energy distributions for the three product ions are plotted in Figure 3. For HCO^+ and CH_4^+, a larger fraction of the available energy is deposited into the internal energy of the photofragments, and the distributions peak near zero. In contrast, the $P(E_T)$ for acetyl ions has a peak at ~0.5

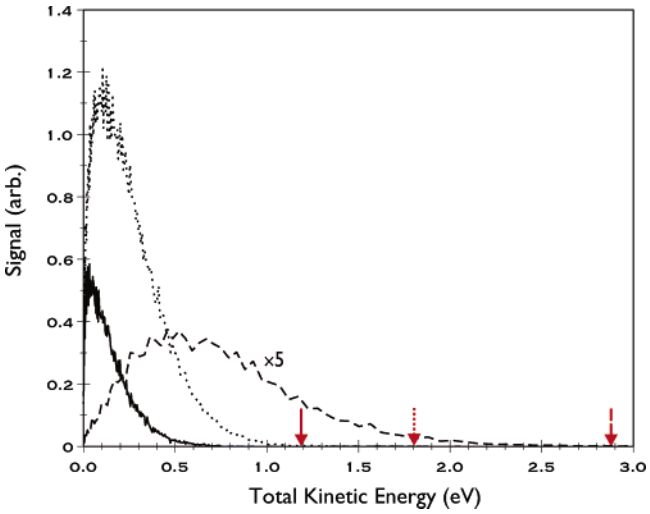

Figure 3. Total translational energy distributions of CH_3CO^+ (dashed line), HCO^+ (dotted line), and CH_4^+ (solid line) ions. The arrows show the available energy for each product ion, and the area under each curve relates to the branching fraction of each product.

TABLE 1: Recoil Anisotropy Parameters for All Fragments[a]

ion	band	β_2	β_4	β_6
CH_3CO^+	origin	0.43	−0.37	0.08
	10_0^1	0.08	−0.30	0.08
	6_0^1, 7_0^1	−0.20	0.01	−0.08
HCO^+	origin	0.85	−0.03	−0.02
CH_4^+	origin	0.52	−0.06	0.01

[a] The uncertainties of reported recoil anisotropy parameters are $\beta_2 \pm 0.1$, $\beta_4 \pm 0.07$, and $\beta_6 \pm 0.01$.

eV and a lower yield of slower fragments, corresponding to the "hole" in the experimental image. The average total translational energy is 0.65, 0.17, and 0.09 eV for the CH_3CO^+, HCO^+, and CH_4^+ channels, respectively. These represent 22, 10, and 8% of the total available energy.

More detailed information on photofragmentation dynamics can be obtained by investigating the angular distribution of the product ions. The angular anisotropy parameters are obtained by fitting the angular distrubutions from the ion images to an even Legendre polynomial expansion including high order terms as follows:

$$I(\theta) \propto 1 + \beta_2 P_2(\cos\theta) + \beta_4 P_4(\cos\theta) + \beta_6 P_6(\cos\theta) \quad (1)$$

where θ is the angle between the laser polarization vector and the recoil velocity vector. The measured anisotropies are listed in Table 1 for all fragments. Although the Legendre polynomial terms up to the eighth order may be required for a thorough description of the angular distribution for this four photon process, we ignore the eighth order term, which is likely to make a negligible contribution. Neglecting any angular modulation by multiphoton ionization processes, the angular distribution for one-photon dissociation should be fitted well including only the second-order Legendre polynomial term. However, as seen in Figure 4, the angular distribution of acetyl ion required higher order Legendre polynomial terms to get an adequate fit. This striking feature is apparent directly in the experimental image showing the four lobes. It implies that more than one photon process is responsible for the angular distribution.

To explore the vibrationally mediated photodissociation dynamics, we also prepared the parent cation using REMPI via the 10_0^1 (55 360 cm^{-1}) and 6_0^1, 7_0^1 (56 195 cm^{-1}) transitions.

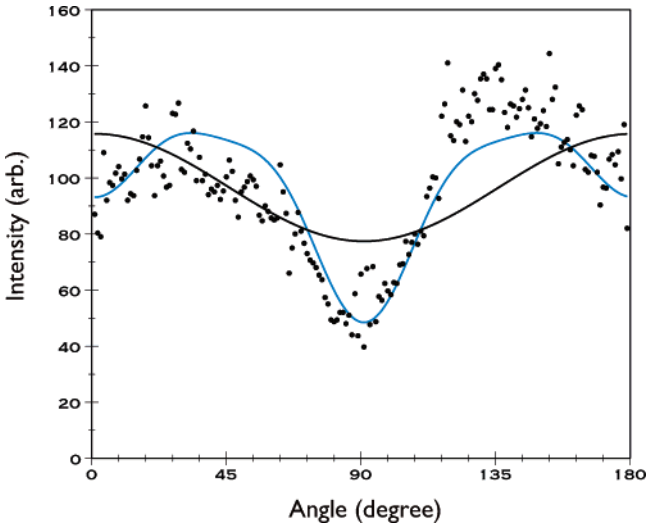

Figure 4. Angular distribution of acetyl ion: solid lines correspond to the best fit without (black) and with (blue) higher order Legendre polynomial terms.

Three product ions (CH_3CO^+, HCO^+ and CH_4^+) were seen at those wavelengths. It is notable that the angular distribution of the acetyl ion becomes isotropic and tends to be perpendicular as the photon energy increases, as shown in Table. 1. The photoelectron image and spectrum at the 10_0^1 transition (Figure 5A) indicates that parent ions are formed predominantly in the $v_{10}^+ = 1$ state, which is in good agreement with the result of Kim and Anderson.[17] Figure 5B displays the photoelectron image and spectrum obtained by REMPI via the 6_0^1, 7_0^1 transition, where there are many rings assigned to several different vibrational states. That is, the parent ions are not well state-selected at this wavelength.

IV. Discussion

Acetaldehyde cations can access two excited states (Ã, B̃) by one-photon absorption in this energy range, and the question of which excited state is predominantly involved in dissociation can be answered by examining the angular distributions of photofragments. As mentioned previously, the interesting angular anisotropy of CH_3CO^+ strongly suggests the presence of multiphoton processes. There have been a few studies of the angular distribution in multiphoton processes recently.[1,21−23] Chichinin and co-workers[24] presented the photofragment angular distribution in the dissociative multiphoton ionization of HCl. Li et al.[4] studied the angular distribution of CO cation multiphoton dissociation. In general, these multiphoton angular distributions could reflect either neutral multiphoton dissociation with subsequent ionization or parent ionization followed by dissociation. However, neutral multiphoton dissociation is not likely in this case, which can be confirmed by measuring the photoelectron image. The kinetic energy release of electrons generated by the two processes is quite different: at the origin band, only 3 meV kinetic energy goes to electrons for the resonant ionization/ion dissociation case, whereas the neutral process with subsequent ionization would be associated with substantial electron kinetic energy. The photoelectron image taken with REMPI through the origin (not shown) displays a strong signal close to zero kinetic energy corresponding to the formation of vibrationless parent ions, consistent with the photoelectron spectroscopy results of Kim et al.[17] This suggests that the product ions result mainly from the dissociation of acetaldehyde cations. The higher order Legendre moments for

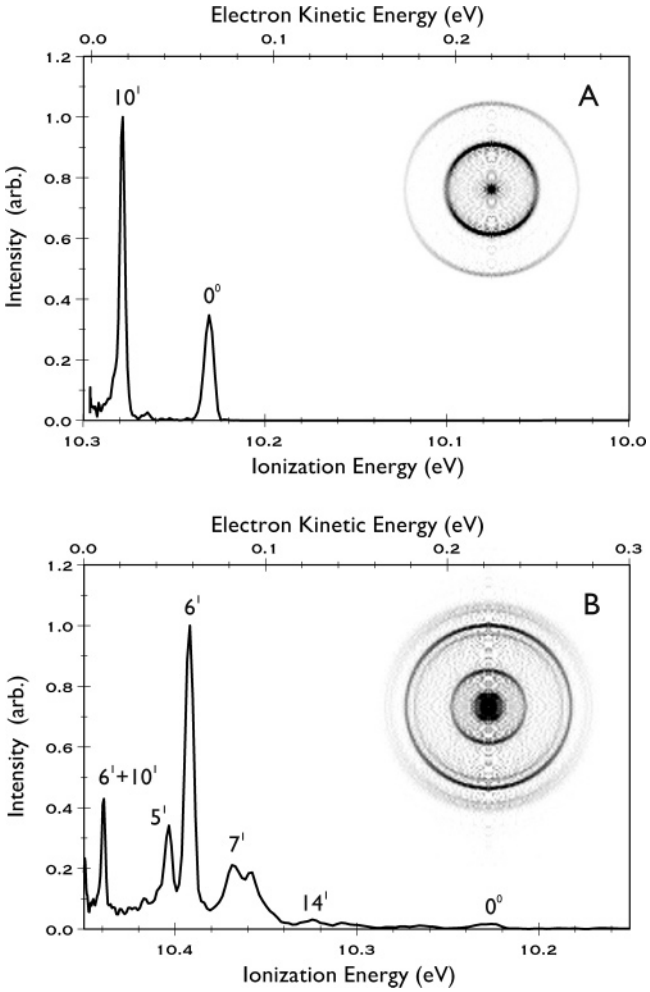

Figure 5. Photoelectron spectra and Abel-inverted images for the photodissociation of acetaldehyde cation produced by 2+1 REMPI through the 10_0^1 (A) and 6_0^1, 7_0^1 (B) bands.

the acetyl ion image thus must reflect alignment of the ion in the (2+1) ionization step.

Although it is not straightforward to quantitatively measure the molecular alignment induced by multiphoton ionization in this complex polyatomic system, in contrast to the diatomic case,[24] a qualitative interpretation may be achieved for the alignment of acetaldehyde cations by analyzing the angular anisotropy parameters. The β_2 value of HCO^+ showing a parallel recoil anisotropy implies that parent ions are spatially aligned with the C−C bond axis almost parallel to the direction of light polarization (**E**), given that all fragments are formed from the same aligned parent ions. The fact that acetaldehyde cations are pre-aligned suggests that the probability of initial excitation to $\tilde{A}^2A''$ (pure perpendicular, out of the CCO plane) is not significant due to the orientation of aligned cations with respect to **E**. In other words, we can speculate that all product ions arise from the initial excitation to the $\tilde{B}^2A'$ state.

The distinct angular distribution of the acetyl ion not only provides reliable evidence of generating aligned parent ions by multiphoton ionization but also indicates that both parallel and perpendicular recoil anisotropies are involved in the H elimination channel. Some of the parallel recoil anisotropy would come from the spatially aligned parent ions, as discussed above. This means that a perpendicular anisotropy might be induced during a dissociation process. According to the discussion of Shin et al.[12] the formation of acetyl and formyl ions is correlated with the dominant initial excitation to the single potential energy surface, the $^2A'$ state. For that case, the angular anisotropy of the acetyl ion would not be much different from that of the formyl ion. To clarify the origin of the two different recoil anisotropies, an ab initio TD−DFT calculation was performed by using the B3LYP/6-31+G(d,p) basis set. The transition dipole moment (μ) to $^2A'$ state was found to lie in the CCO molecular plane, and the recoil anisotropy was determined by the angle (α) between the direction of μ and the recoil direction of a fragment, as described by the well-known $\beta = 2P_2(\cos\alpha)$ expression. Assuming a fast dissociation process (ignoring the nonaxial recoil dynamics), the angle α can be estimated by considering the asymptotic recoil direction of interest as the corresponding internuclear axis (see the inset in Figure 1). The estimated values of α formed by the C−H bond in a formyl group and the C−C bond are about 110° ($\beta_{cal} \approx -0.65$) and 136° ($\beta_{cal} \approx 0.55$), respectively. This implies that the angular anisotropy of the acetyl ion in dissociation is more perpendicular relative to that of the formyl ion even though both the H elimination and the C−C cleavage happen through the same initial excitation. The reason for having an estimated value lower than the experimental β for HCO^+ (0.85) could be that the angular modulation by spatially aligned parent ions was not considered. The angular distribution for CH_4^+, with the relatively lower β_2 value, cannot be easily rationalized with a simple picture owing to either the H intramolecular rearrangement (hydrogen scrambling) or the possible partial contribution from a roaming mechanism.

The angular distribution of the acetyl ions varies with a well-characterized excitation in a specific vibrational mode as indicated in Table 1. At the 10_0^1 transition, its vibrational motions (CH_3 rocking and CCO bending) could interfere with the appearance of the alignment of the acetaldehyde cation. However, the aligned parent ions are still seen, as evidenced by the large value of β_4. In contrast, the angular distribution at the 6_0^1, 7_0^1 band has a small perpendicular anisotropy with a β_4 parameter near zero. Vibrational motions in several modes probably wash out the molecular alignment effect, resulting in the formation of parent ions with an angular distribution that is nearly isotropic. Therefore, the overall angular distribution may be mainly attributed to the one-photon dissociation of parent cations, in agreement with the above explanation of a perpendicular component for the H elimination channel.

The results of the translational energy distribution measurements are consistent with those reported by Johnson and coworkers[11] at lower resolution. These features of the translational energy distributions for HCO^+ and CH_4^+ (Figure 3) are often interpreted as a signature of barrierless statistical dissociation from the ground state.[25] The small partitioning (8−10%) into product translational energy is not consistent with the direct dissociation along a repulsive excited state or predissociating state. Therefore, it can be proposed that these products arise from the ground electronic state following internal conversion as argued by Johnson et al. For the formation of CH_4^+, one might suspect the dissociation to occur over a barrier. The observed $P(E_T)$ of CH_4^+ implies that the barrier must be very small, unlike the photodissociation of neutral acetaldehyde. An alternative explanation to account for the low translational energy and high internal energy in this channel is the possibility of a "roaming" mechanism[26] involving methyl radicals, co-fragments of formyl ions. In this picture, methyl radicals are nearly lost via barrierless dissociation but return to effect intramolecular proton abstraction forming highly excited CH_4^+. In an analogous recent study of acetaldehyde photodissociation,

the role of a roaming mechanism in the CH_3 + HCO channel was proposed to form the final products, CH_4 and CO.[27]

The peak of $P(E_T)$ for CH_3CO^+ is away from zero energy. This could be due to a secondary dissociation pathway involving the fragmentation of highly excited CH_3CO^+. However, this explanation can be ruled out because there is no evidence of opening of the secondary channel (i.e., no CH_3^+). Another possibility is the presence of an exit barrier for the H elimination channel. To date, the measured appearance energy (AE) of the acetyl ions ranges from 10.67 to 10.90 eV,[28−30] which represents either a nearly zero or very small barrier. Some theoretical studies[31,32] reported that a small exit barrier (∼0.1 eV) exists for this channel. Johnson and co-workers[11] found that the translational energy partitioning of the total available energy, $\langle E_{trans}\rangle/\langle E_{avail}\rangle$ is ∼22 and 11% for the acetyl and formyl ions, respectively, which is consistent with our results. They found those values were in accord with statistical predictions and concluded that those product ions occurs via internal conversion followed by dissociation on the ground state. The larger translational energy release for the H atom loss channel is largely owing to the absence of rotational degrees of freedom for that fragment.

V. Conclusion

We report here the translational energy and angular distributions of fragments in the photodissociation of acetaldehyde cations using DC slice imaging. The peculiar angular distribution of acetyl ions having a large value of β_4 anisotropy parameter supports the suggestion that parent ions produced by REMPI via the origin band are predominantly aligned parallel to the polarization direction of light in the multiphoton ionization process. The spatially aligned parent cation is mostly excited to the $\tilde{B}$ state and dissociates. However, the spatial alignment effect is diminished when dissociation occurs through parent ions populated in many vibrational excited states.

Acknowledgment. This work was supported by the National Science Foundation under award number CHE-0415393.

References and Notes

(1) Vieuxmaire, O. P. J.; Nahler, N. H.; Jones, J. R.; Dixon, R. N.; Ashfold, M. N. R. *Mol. Phys.* **2005**, *103*, 2437.
(2) Beckert, M.; Greaves, S. J.; Ashfold, M. N. R. *Phys. Chem. Chem. Phys.* **2003**, *5*, 308.
(3) Aguirre, F.; Pratt, S. T. *J. Chem. Phys.* **2003**, *118*, 6318.
(4) Li, W.; Lahankar, S. A.; Huang, C.; Shternin, P. S.; Vasyutinskii, O. S.; Suits, A. G. *Phys. Chem. Chem. Phys.* **2006**, *8*, 2950.
(5) Chang, C.; Luo, C. Y.; Liu, K. *J. Phys. Chem. A* **2005**, *109*, 1022.
(6) Kim, M. H.; Leskiw, B. D.; Suits, A. G. *J. Phys. Chem. A* **2005**, *109*, 7839.
(7) Kim, M. H.; Shen, L.; Suits, A. G. *Phys. Chem. Chem. Phys.* **2006**, *8*, 2933.
(8) Jochims, H. W.; Lohr, W.; Baumgärtel, H. *J. Chem. Phys.* **2003**, *118*, 6318.
(9) Fisanick, G. J.; Eichelberger, T. S.; Heath, B. A.; Robin, M. B. *Chem. Phys. Lett.* **1978**, *54*, 594.
(10) Bombach, R.; Stadelmann, J. P.; Vogt, J. *Chem. Phys.* **1981**, *60*, 293.
(11) Johnson, K.; Powis, I.; Danby, C. J. *Chem. Phys.* **1982**, *70*, 329.
(12) Shin, S. K.; Kim, B.; Haldeman, J. G.; Han, S. J. *J. Chem. Phys.* **1996**, *100*, 8280.
(13) Buntine, M. A.; Metha, G. F.; McGilvery, D. C.; Morrison, R. J. S. *J. Mol. Spectrosc.* **1994**, *165*, 12.
(14) Shand, N. C.; Ning, C. N.; Pfab, J. *Chem. Phys. Lett.* **1995**, *247*, 32.
(15) Meyer, H. *Chem. Phys. Lett.* **1996**, *262*, 603.
(16) Kim, Y.; Fleniken, J.; Meyer, J. *Chem. Phys.* **1998**, *109*, 3401.
(17) Kim, H. T.; Anderson, S. L. *J. Chem. Phys.* **2001**, *114*, 3018.
(18) NIST standard reference database, http://webbook.nist.gov/chemistry/.
(19) Townsend, D.; Minitti, M. P.; Suits, A. G. *Rev. Sci. Instrum.* **2003**, *74*, 2530.
(20) Li, W.; Chambreau, S. D.; Lahankar, S. A.; Suits, A. G. *Rev. Sci. Instrum.* **2005**, *76*, 063106.
(21) Cosofret, B. R.; Lambert, H. M.; Houston, P. L. *J. Chem. Phys.* **2002**, *117*, 8787.
(22) Manzhos, S.; Romanescu, C.; Loock, H.-P.; Underwood, J. G. *J. Chem. Phys.* **2004**, *121*, 11802.
(23) Dixon, R. N. *J. Chem. Phys.* **2005**, *122*, 194302.
(24) Chichinin, A. I.; Shternin, P. S.; Gödecke, N.; Kauczok, S.; Maul, C.; Vasyutinskii, O. S.; Gericke, K. H. *J. Chem. Phys.* **2006**, *125*, 034310.
(25) Blank, D. A.; North, S. W.; Stranges, D.; Suits, A. G. *J. Chem. Phys.* **1997**, *106*, 539.
(26) Townsend, D.; Lahankar, S. A.; Lee, S. K.; Chambreau, S. D.; Suits, A. G.; Zhang, X.; Rheinecker, J.; Harding, L. B.; Bowman, J. M. *Science* **2004**, *306*, 1158.
(27) Houston, P. L.; Kable, S. H. *Proc. Natl. Acad. Sci.* **2006**, *103*, 16079.
(28) Krässig, R.; Reinke, D.; Baumgärtel, H.; Bunsenges, B. *Phys. Chem.* **1974**, *78*, 425.
(29) Staley, R. H.; Wieting, R. D.; Beauchamp, H. *J. Am. Chem. Soc.* **1977**, *99*, 5964.
(30) Traeger, J. C.; McLoughlin, R. G.; Nicholson, A. J. C. *J. Am. Chem. Soc.* **1982**, *104*, 5318.
(31) Radom, L. *Int. J. Mass Spectrom. Ion Processes* **1990**, *101*, 209.
(32) Bertrand, W.; Bouchoux, G. *Rapid Commun. Mass Spectrom.* **1998**, *12*, 1697.